ChemComm

Accepted Manuscript

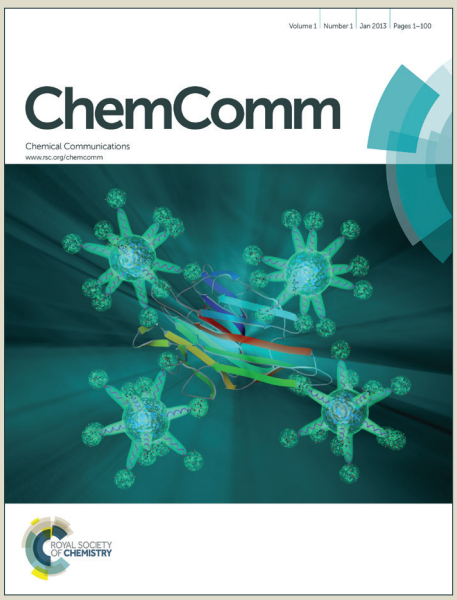

ROYAL SOCIETY OF CHEMISTRY

www.rsc.org/chemcomm

Chemical Communications RSCPublishing

COMMUNICATION

An activatable, polarity dependent, dual-luminescent imaging agent with long luminescence lifetime

Cite this: DOI: 10.1039/x0xx00000x

Marcus T.M. Rood,[a] Maria Oikonomou,[b] Tessa Buckle,[a] Marcel Raspe,[c] Yasuteru Urano,[d] Kees Jalink,[c] Aldrik H. Velders[a,b] and Fijs W.B. van Leeuwen[a,b]

Received 00th January 2012,
Accepted 00th January 2012

DOI: 10.1039/x0xx00000x

www.rsc.org/

In this proof-of-concept study, a new activatable imaging agent based on two luminophores and two different quenching mechanisms is reported. Both partial and total activation of the luminescence signal can be achieved, either in solution or *in vitro*. Bond cleavage makes the compound suitable for luminescence lifetime imaging.

Luminescence imaging is widely used in molecular cell biology and the technology is more and more explored in the clinical setting *e.g.* for surgical guidance.[1] While the emission of luminophores can be used directly, the (photo)physical interactions between different luminescent compounds also has value in diagnostic applications.[2] Uniquely, disturbance of the interaction between a luminophore and a quencher, or chemical modification of a luminophore, can generate disease-specific signals.[3] Generally an activatable approach provides a measure for enzymatic activity.[4]

Organic dyes, which are most commonly explored as activatable imaging agents, are prone to interferences from autofluorescence. This disturbance can be minimized by tailoring the wavelengths towards the far-red and near-infrared window where the autofluorescence is minimal.[5] Alternatively, luminophores may be designed to have a large Stokes shift (> 100 nm) to obtain a peak intensity that lies beyond the spectral range where autofluorescence generally occurs.[1] Luminescence lifetime may also help to separate exogenous from endogenous signals.[6]

We reasoned that the specificity of an activatable imaging agent can be improved by exploiting luminescence lifetimes that exceed those of endogenous molecules (0.1-7 ns).[7] Added advantages of phosphorescent transition complexes are their high photostability, large Stokes shift, and inability of self-quenching.[8] Previously some efforts have been made to use ruthenium or iridium complexes for imaging,[5, 9] and and a few ruthenium complexes have been investigated that give a change in luminescence lifetime (τ > 10 ns).[10] Iridium complexes allow two types of quenching: First, Förster Resonance Energy Transfer (FRET) or triplet-triplet energy transfer from an iridium complex to an organic moiety, thereby quenching the iridium-based phosphorescence.[11, 12] Second, iridium atoms can induce spin-orbit coupling on other luminophores, quenching the other dye.[12] In contrast to effective distances in FRET (up to 10 nm),[13] distances in spin-orbit coupling effects are confined to 1 nm.[14] Although spin-orbit coupling is considered a drawback in the efficiency of LEDs containing transition metals,[15] we aim to exploit this effect, in combination with FRET, as basis to generate a new class of activatable imaging agents.

The combination of luminescence signal activation and luminescence lifetime imaging was examined using a $Ir(ppy)_3$ complex and a Cy5 dye to combine the desired effects of both imaging strategies in a dual-luminescent imaging agent.

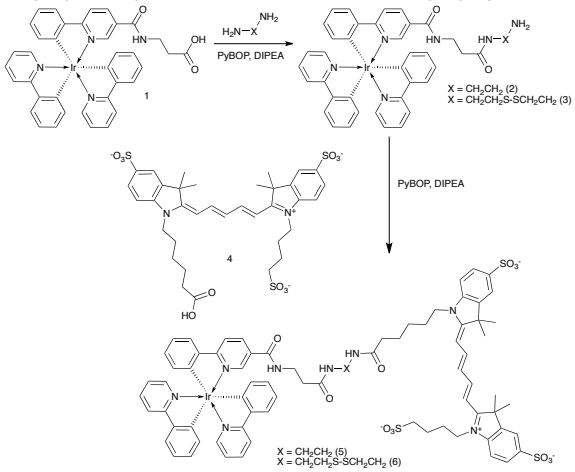

Scheme 1. Synthesis of $Ir(ppy)_3$-Cy5 compounds with different linkers

After synthesis of the $Ir(ppy)_3$-complex (**1**), a suitable linker was attached (**2-3**). Excess linker was used to minimize dimer formation (Scheme 1, see Supplementary Information (SI) for detailed experimental section). This resulted in yields of 42% (**2**) and 56%

(**3**). Cy5 was chosen as FRET acceptor because of its spectral overlap with $Ir(ppy)_3$ (Figure 1A) and high extinction coefficient ($\varepsilon = 2.5*10^5$). Compounds **5** and **6** were made to provide both stable and activatable derivatives of the conjugate. Conjugation with Cy5 (**4**) was achieved using standard peptide coupling chemistry. After purification, in both cases a blue/green solid was obtained in yields of 64% (**5**) and 33% (**6**).

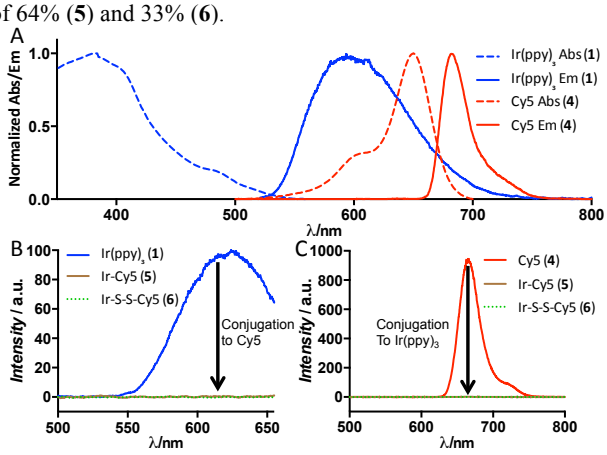

Figure 1. A) Normalized absorption and emission spectra of $Ir(ppy)_3$ and Cy5 in PBS showing the spectral overlap. B) Emission of equimolar solutions of **1**, **5** and **6** with 457 nm excitation and C) emission of equimolar solutions of **4**, **5** and **6** with 627 nm excitation in PBS

When $Ir(ppy)_3$ (**1**) is excited, it undergoes rapid inter-system crossing to a triplet excited state and from there emits phosphorescent light ($\varepsilon = 9*10^3$; $\Phi = 0.12$ (DMSO)).[16] FRET from $Ir(ppy)_3$ to Cy5 prevented $Ir(ppy)_3$ emission in **5** and **6** in phosphate buffered saline (PBS) (Figure 1B). Independent of the solvent, the $Ir(ppy)_3$ emission remained fully quenched indicating energy transfer occurs from $Ir(ppy)_3$ to the Cy5 singlet excited state by FRET; we calculated the Förster distance between these luminophores to be 4.8 nm (see SI, p. 5).[17] The donor-acceptor distances in our compounds fall well within this distance, allowing for efficient quenching.

The spin-orbit coupling induced by the iridium atom was used to quench emission of Cy5 efficiently (Figure 1C) by allowing energy transfer from the singlet excited state of Cy5 to a non-emissive triplet excited state of Cy5 (Figure S1). Regardless the excitation wavelength (405 or 633 nm), at 77 K the emission spectra of **5** showed two peaks at 760 and 840 nm (Figure S3). These peaks correspond to the previously reported triplet state emission of Cy5.[18] Since in **5** and **6** the emission of both luminophores is substantially quenched (>99.7 %), we state that in PBS the luminescence is in the off-state when the luminophores are conjugated.

The difference in distance dependence between the two quenching mechanisms was used to largely mitigate spin-orbit coupling, while leaving FRET intact. Using MeOH as co-solvent increased the solvation of **5** and **6** and this resulted in Cy5 singlet emission at 670 nm upon excitation of $Ir(ppy)_3$ (Figure S2). In the absorption spectra, changing to a more apolar solvent leads to a decrease in the peak (610 nm) that indicates stacking interactions (Figure S4B). This conformational change resulted in a 30-fold increase of Cy5 fluorescence intensity (Figure S4C), while the $Ir(ppy)_3$ emission remained quenched. The rotational freedom of the molecules, however, seems to prevent complete signal restoration. The triplet emission caused by spin-orbit coupling in **5** (observed at 77 K in H_2O) disappeared upon reduction in polarity, also indicating a change in the interaction between Cy5 and the Ir atom (Figure S3A). Lastly ROESY spectra in CD_3OD did not reveal close distance correlations between Cy5 and $Ir(ppy)_3$ (SI, Appendix).

Similar to the use of MeOH, micelles of SDS were able to increase the Cy5 luminescence intensity, providing a model system for interactions with the cell membrane. Only above the critical micelle concentration of 1.2 mM[19] an increase of Cy5 fluorescence intensity was observed (Figure S5). In line with these findings, interaction of **5** (the uncleavable derivative; Figure 2) or **6** (Figure S6) with cell membranes provided a detectable Cy5 emission; $Ir(ppy)_3$ emission remained quenched.

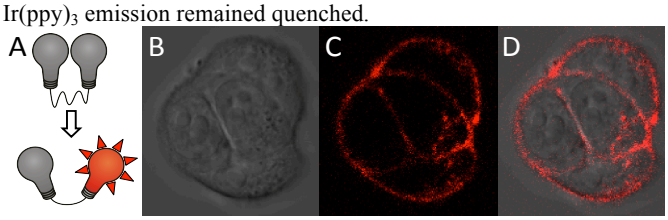

Figure 2. A) Schematic representation of partial activation by conformational change of the probe. B-D) Confocal microscope image of 4T1 cells after 1h incubation with **5** at 4°C. B) Differential interference contrast, C) Cy5, D) overlay.

In **6**, the quenching of both $Ir(ppy)_3$ and Cy5 can be fully undone by cleavage of the connective bond between the two dyes (Figure 3A). To study the full activation, the disulfide bond of **6** (a model system for cleavage) was initially cleaved using cysteamine (Scheme S2). In MeOH:PBS 4:1, after 1h at RT, the cleavage reaction induced by an excess of cysteamine yielded an intensity increase of both $Ir(ppy)_3$ phosphorescence (100-fold increase, Figure 3C) and Cy5 fluorescence (a further 3-fold increase on the 30-fold increase caused by the solvent, making a total 90-fold, Figure 3D). In PBS a 200-fold increase of Cy5 fluorescence intensity was observed (Figure S7). After cleavage the end prodcuts were analyzed using HPLC and mass spectrometry (Figures S8 and S9).

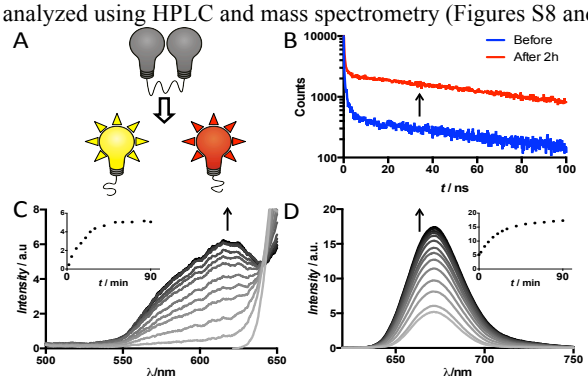

Figure 3. A) Schematic representation of disulfide cleavage, B) difference in luminescence decay before and after cleavage in solution, C) increase of luminescence of $Ir(ppy)_3$ and D) Cy5 upon cleavage. Insets in C) and D) are the change of peak height over time.

In vitro evaluation of the disulfide bond cleavage was performed in the 4T1 murine breast tumor cell line. After passive cellular internalization at 37°C, Ir-S-S-Cy5 (**6**) was confined in the lysosomes of the cell, where the disulfide bond was reduced by a redox enzyme or an intracellular thiol.[20] We observed activation of both $Ir(ppy)_3$ and Cy5 in the lysosomes (Figure 4; Figure S10) and even when a high concentration (5 µM) of **6** surrounded the cells, only the cleaved components were visible (Figure S11). No $Ir(ppy)_3$ signal activation was observed when cells were incubated at 37°C with **5** (Figure S12).

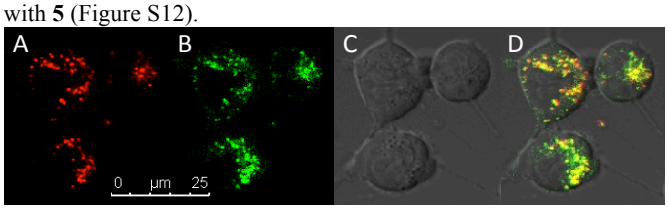

Figure 4. Confocal microscope images of 4T1 cells after 24h incubation with **6** at 37°C. A) Cy5 in red, B) $Ir(ppy)_3$ in green, C) differential interference contrast, D) overlay of all channels. Yellow indicates overlay of red and green.

Luminescence lifetime measurements showed minor differences between the iridium complexes **1**, **2**, and **3** (Table 1). Conjugation

with Cy5 (**4**) drastically shortened the lifetime. A short-lived species (τ < 1 ns), representative for residual Cy5 emission, accounted for a large part of the total emission at 600 nm; 89 % in **5** and 91 % in **6** (Figure S13). After cleavage, there is a relative large increase of long-lifetime emission (Figure 3B), indicating re-activation of $Ir(ppy)_3$ phosphorescence. Activation effects observed in solution were confirmed *in vitro* by fluorescence lifetime imaging microscopy (FLIM) using two different cell lines, 4T1 and U2OS. Results were independent of cell type (Figures 5 and S14). With **5** (uncleavable), the lifetime was short, while after activation of **6** (cleavable) the lifetime increased to 90 ns, similar to control experiments (Figure S14A). The change in lifetime seen with FLIM provides a clear measure of the *in vitro* activation. Unfortunately, the suboptimal filter cube also allows for some background, giving an average in lifetime signal. A time-gated approach, which was not possible in our set-up, might prevent this.

Table 1. Luminescence lifetimes of selected compounds in MeOH:PBS 4:1

Compound	**1**	**2**	**3**	**4**[a]	**5**	**6**
τ fast (ns)	N.A.[b]	N.A.[b]	N.A.[b]	1.0	0.55 (89 %)[c]	0.35 (95 %)[c]
τ slow (ns)	97.2	79.4	87.5	N.A.[b]	78.6	91.1
Average τ (ns)	97.2	79.4	87.5	1.0	9.1	4.9

[a] Emission measured at 680 nm [b] Not applicable [c] Relative signal contribution

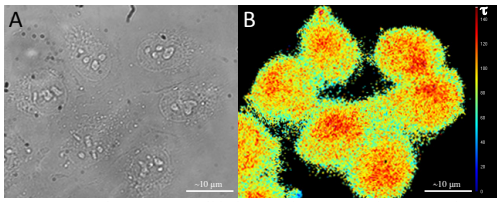

Figure 5. Fluorescence lifetime microscopy images of U2OS cells after 24h incubation with **6** at 37°C using a CFP/YFP filter cube (excitation 436/12 & 500/20, dichroic 445 & 515, emission 467/37 & 545/45). A) Transmission, B) lifetime, the scale of the lifetimes is depicted on the right side (0-150 ns).

The lifetime technology proves to be a promising tool to analyze variations in cellular function related to disease progression.[7, 21] Although the here-described disulfide cleavage procedure is not disease-specific; every cell is able to cleave disulfide bonds,[20] it acts as a model system. In the future, derived activatable lifetime agents can in theory be used to detect expression levels of disease-related enzymes. When more disease-specific probes for FLIM are available, the scope of lifetime imaging may be expanded from *in vitro* to *in vivo* applications and maybe even to applications in image guided surgery.[22]

Conclusions

To conclude, two different quenching mechanisms were used to generate a dual-luminescent activatable (long) lifetime imaging agent based on Cy5 and $Ir(ppy)_3$ (**6**). In our view activatable long lifetime imaging agents provide a promising tool for future molecular imaging related to disease progression, complementary to intensity-based fluorescence detection.

Notes and references

[a] Interventional Molecular Imaging Laboratory, Department of Radiology, Leiden University Medical Center, Leiden (The Netherlands).
[b] Laboratory of BioNanoTechnology, Wageningen University, Wageningen (The Netherlands).
[c] Division of Cell Biology I, Netherlands Cancer Institute, Amsterdam (The Netherlands).
[d] Laboratory of Chemical Biology & Molecular Imaging, Graduate School of Medicine, The University of Tokyo, Tokyo (Japan).

This research was supported by an NWOnano-Grant (STW 11435; F.v.L.). The authors would like to thank A. Bunschoten, D. van Willigen and P. Steunenberg for kindly supplying compounds. We also thank P. Navarro, P. Chin, S. van der Wal and H. Tanke for fruitful discussions.

Electronic Supplementary Information (ESI) available: Synthesis, *in vitro* studies, Förster distance calculation, and supplementary images. See DOI: 10.1039/c000000x/

1 P. T. K. Chin, M. M. Welling, S. C. J. Meskers, R. A. V. Olmos, H. Tanke and F. W. B. van Leeuwen, *European Journal of Nuclear Medicine and Molecular Imaging*, 2013, **40**, 1283.
2 R. Weissleder and V. Ntziachristos, *Nature Medicine*, 2003, **9**, 123.
3 Y. Urano, *Current Opinion in Chemical Biology*, 2012, **16**, 602; J. F. Lovell and G. Zheng, *Journal of Innovative Optical Health Sciences*, 2008, **1**, 45.
4 C. W. Huang, Z. B. Li and P. S. Conti, *Bioconjugate Chemistry*, 2012, **23**, 2159; C. H. Tung, U. Mahmood, S. Bredow and R. Weissleder, *Cancer Research*, 2000, **60**, 4953; Y. Urano, M. Sakabe, N. Kosaka, M. Ogawa, M. Mitsunaga, D. Asanuma, M. Kamiya, M. R. Young, T. Nagano, P. L. Choyke and H. Kobayashi, *Science Translational Medicine*, 2011, **3**, 110ra119.
5 G. Zhang, H. Zhang, Y. Gao, R. Tao, L. Xin, J. Yi, F. Li, W. Liu and J. Qiao, *Organometallics*, 2014, **33**, 61.
6 R. Alford, M. Ogawa, M. Hassan, A. H. Gandjbakhche, P. L. Choyke and H. Kobayashi, *Contrast Media & Molecular Imaging*, 2010, **5**, 1.
7 M. Y. Berezin and S. Achilefu, *Chemical reviews*, 2010, **110**, 2641.
8 A. Ruggi, C. Beekman, D. Wasserberg, V. Subramaniam, D. N. Reinhoudt, F. W. B. van Leeuwen and A. H. Velders, *Chemistry-a European Journal*, 2011, **17**, 464.
9 P. Steunenberg, A. Ruggi, N. S. van den Berg, T. Buckle, J. Kuil, F. W. B. van Leeuwen and A. H. Velders, *Inorg. Chem.*, 2012, **51**, 2105; L. Murphy, A. Congreve, L.-O. Palsson and J. A. G. Williams, *Chemical Communications*, 2010, **46**, 8743; L. Xiong, Q. Zhao, H. Chen, Y. Wu, Z. Dong, Z. Zhou and F. Li, *Inorg. Chem.*, 2010, **49**, 6402; G. Li, Y. Chen, J. Wu, L. Ji and H. Chao, *Chemical Communications*, 2013, **49**, 2040; A. Ruggi, F. W. B. van Leeuwen and A. H. Velders, *Coordination Chemistry Reviews*, 2011, **255**, 2542.
10 W. Zhong, P. Urayama and M. A. Mycek, *Journal of Physics D-Applied Physics*, 2003, **36**, 1689; E. Baggaley, M. R. Gill, N. H. Green, D. Turton, I. V. Sazanovich, S. W. Botchway, C. Smythe, J. W. Haycock, J. A. Weinstein and J. A. Thomas, *Angew Chem Int Ed Engl*, 2014, **53**, 3367.
11 H. Y. Shiu, M. K. Wong and C. M. Che, *Chemical Communications*, 2011, **47**, 4367.
12 R. D. Costa, F. J. Cespedes-Guirao, H. J. Bolink, F. Fernandez-Lazaro, A. Sastre-Santos, E. Orti and J. Gierschner, *Journal of Physical Chemistry C*, 2009, **113**, 19292; A. A. Rachford, R. Ziessel, T. Bura, P. Retailleau and F. N. Castellano, *Inorg. Chem.*, 2010, **49**, 3730.
13 E. A. Jares-Erijman and T. M. Jovin, *Nature Biotechnology*, 2003, **21**, 1387.
14 M. Rae, A. Fedorov and M. N. Berberan-Santos, *Journal of Chemical Physics*, 2003, **119**, 2223.
15 C. Rothe, S. King and A. Monkman, *Nature Materials*, 2006, **5**, 463.
16 J. Kuil, P. Steunenberg, P. T. K. Chin, J. Oldenburg, K. Jalink, A. H. Velders and F. W. B. van Leeuwen, *ChemBioChem*, 2011, **12**, 1896.
17 G. Horvath, M. Petras, G. Szentesi, A. Fabian, J. W. Park, G. Vereb and J. Szollosi, *Cytometry Part A*, 2005, **65A**, 148.
18 Z. X. Huang, D. M. Ji, A. D. Xia, F. Koberling, M. Patting and R. Erdmann, *Journal of the American Chemical Society*, 2005, **127**, 8064.
19 R. J. Williams, J. N. Phillips and K. J. Mysels, *Transactions of the Faraday Society*, 1955, **51**, 728.
20 G. Saito, J. A. Swanson and K. D. Lee, *Advanced Drug Delivery Reviews*, 2003, **55**, 199.
21 W. Becker, *Journal of Microscopy*, 2012, **247**, 119.
22 Y. Sun, J. E. Phipps, J. Meier, N. Hatami, B. Poirier, D. S. Elson, D. G. Farwell and L. Marcu, *Microscopy and Microanalysis*, 2013, **19**, 791.